



---

*Research article*

## Stochastic solitons of a short-wave intermediate dispersive variable (SI<sub>d</sub>V) equation

Shabir Ahmad<sup>1</sup>, Saud Fahad Aldosary<sup>2,\*</sup> and Meraj Ali Khan<sup>3</sup>

<sup>1</sup> Department of Mathematics, University of Malakand, Chakdara, Dir Lower, Khyber Pakhtunkhwa, Pakistan

<sup>2</sup> Department of Mathematics, College of Science and Humanities in Alkharj, Prince Sattam bin Abdulaziz University, Alkharj 11942, Saudi Arabia

<sup>3</sup> Department of Mathematics and Statistics, College of Science, Imam Mohammad Ibn Saud Islamic University (IMSIU), P. O. Box-65892, Riyadh 11566, Saudi Arabia

\* **Correspondence:** Email: [sau.aldosary@psau.edu.sa](mailto:sau.aldosary@psau.edu.sa).

**Abstract:** It is necessary to utilize certain stochastic methods while finding the soliton solutions since several physical systems are by their very nature stochastic. By adding randomness into the modeling process, researchers gain deeper insights into the impact of uncertainties on soliton evolution, stability, and interaction. In the realm of dynamics, deterministic models often encounter limitations, prompting the incorporation of stochastic techniques to provide a more comprehensive framework. Our attention was directed towards the short-wave intermediate dispersive variable (SI<sub>d</sub>V) equation with the Wiener process. By integrating advanced methodologies such as the modified Kudrayshov technique (KT), the generalized KT, and the sine-cosine method, we delved into the exploration of diverse solitary wave solutions. Through those sophisticated techniques, a spectrum of the traveling wave solutions was unveiled, encompassing both the bounded and singular manifestations. This approach not only expanded our understanding of wave dynamics but also shed light on the intricate interplay between deterministic and stochastic processes in physical systems. Solitons maintained stable periodicity but became vulnerable to increased noise, disrupting predictability. Dark solitons obtained in the results showed sensitivity to noise, amplifying variations in behavior. Furthermore, the localized wave patterns displayed sharp peaks and periodicity, with noise introducing heightened fluctuations, emphasizing stochastic influence on wave solutions.

**Keywords:** KdV equation; Wiener process; soliton

**Mathematics Subject Classification:** 35C05, 35C07, 35C08

---

## 1. Introduction

Over the past several years, integrable systems (IS) have been a captivating field of research for their applications in science and engineering [1]. The unique features of these IS and their wide range of implications make them intriguing. In the context of science, IS provides insightful solutions and analytical methods that improve our understanding of complex processes [2]. Moreover, they serve as important tools for optimizing processes and addressing intricate problems in engineering applications. Li and Tian systematically solved the Cauchy problem of the general  $n$ -component nonlinear Schrödinger equations based on the Riemann-Hilbert method, and given the  $N$ -soliton solutions. Moreover, they proposed a conjecture about the law of nonlinear wave propagation [3]. With respect to soliton resolution conjecture, Li, Tian, Yang, and Fan have done some interesting work in deriving the solutions of Wadati-Konno-Ichikawa equation, complex short pulse equation and short pulse equation with the help of Dbar-steepest descent method [4]. They solved the long-time asymptotic behavior of the solutions of these equations, and proved the soliton resolution conjecture and the asymptotic stability of solutions of these equations [5–7].

Throughout the recent years several useful works have been observed in the literature. For instance, exploring wave phenomena across various disciplines such as oceanography, acoustics, and hydrodynamics is achieved through an extended coupled (2+1)-dimensional Burgers system [8]. Investigation of ultra-short optical pulses within a birefringent fiber employs a generalized coupled Hirota system, incorporating singular manifold analysis and symbolic computation [9, 10]. The study of solitons and generalized Darboux transformations is conducted for the Ablowitz–Ladik equation within an electrical lattice [11]. Analysis of multi-pole solitons is carried out in an inhomogeneous multi-component nonlinear optical medium [12]. Auto-Bäcklund transformations and soliton solutions on non-zero backgrounds are explored for a (3+1)-dimensional Korteweg-de Vries-Calogero-Bogoyavlenskii-Schif equation in a fluid medium [13]. Some more works include [14–18].

The study of IS became significant when studying famous examples like the Korteweg-de-Vries (KdV) equation [19]. During past years, researchers have focused on the KdV equation [20]. The integrability of this system makes it a noteworthy illustration of an integrable system, connecting theoretical phenomena with practical applications [21]. Two-layer liquid and lattice considerations are investigated through a (3+1)-dimensional generalized Yu-Toda-Sasa-Fukuyama system [22]. Similarly, oceanic shallow-water investigations are conducted on a generalized Whitham-Broer-Kaup-Boussinesq-Kupershmidt system [23]. Recent works include the bifurcations and chaos analysis of several PDEs. For example, the investigation delves into the dynamic behavior and the emergence of multiple optical solitons in optical fibers through the fractional Ginzburg–Landau equation incorporating  $\beta$ -derivative terms [24]. Analyzing bifurcation phenomena, the study explores optical soliton perturbations employing the Radhakrishnan–Kundu–Lakshmanan equation [25]. Investigating bifurcations and the existence of dispersive optical solitons, the research focuses on the nonlinear Schrödinger–Hirota equation within DWDM networks [26]. Additionally, examining bifurcation dynamics and the formation of multiple solitons, attention is given to birefringent fibers utilizing the coupled Schrödinger–Hirota equation [27]. The basic version of KdV equation is expressed as:

$$\mathcal{G}_t + 6\mathcal{G}\mathcal{G}_x + \mathcal{G}_{xxx} = 0. \quad (1.1)$$

In the field of science, the study of nonlinear waves leads to the emergence of the KdV equation, giving

a mathematical framework for analyzing phenomena like solitons. These solitary waves solutions find implications in different physical contexts, containing fluid mechanics and plasma physics, where the characteristics are expressed by the KdV equation. The integrability of the KdV equations permits researchers to attain closed form solutions, leading to a more profound comprehension of the given behavior. For Eq (1.1), the order one soliton is expressed as:

$$\mathcal{G}(x, t) = \frac{\beta}{2} \operatorname{sech}^2 \left[ \frac{\sqrt{\beta}}{2} (x - \beta t - x_0) \right]. \quad (1.2)$$

A remarkable recent finding in the field of nonlinear PDEs is the SIdV equation. The SIdV equation portrays an important extension of the famous KdV equation, renowned for its capacity to study different physical phenomena, specifically those related to waves in shallow water. The unique combination of the short wave and intermediate dispersive properties in the SIdV equation is what makes it so fascinating. By involving features from the both regimes, the SIdV acts a link between the KdV equation and the conventional short wave, offering a more complex point of view. Compared to the standard short wave equations or KdV equation, the equation's applicability is increased by its special mix of short wave and intermediate dispersive features, which allows it to simulate a wider range of wave events. The equation of the SIdV is given as [28]:

$$\mathcal{G}_t + \left( \frac{2\mathcal{G}_{xx}}{\mathcal{G}} \right) \mathcal{G}_x = \mathcal{G}_{xxx}. \quad (1.3)$$

The SIdV equation is interesting owing to the way its intermediate features and short wave dispersive characteristics are structured. Due to the capacity of the SIdV equation to capture intricate wave dynamics that other models may ignore, the SIdV equation is desirable to both scholars and practitioners. Exploring the SIdV equation thereby enriches our knowledge of nonlinear wave process and offers new prospects to usage in fluid and plasma physics, among other fields. Its role as a generalized KdV equation provides the basis for a better understanding of nonlinear PDEs and their applications. The literature [29, 30] provides documentation of several studies on the SIdV equation. The authors in [31] constructed the following version of SIdV equation as:

$$\mathcal{G}_t + \left( 3(1 - \varrho)\mathcal{G} + (1 + \varrho)\frac{\mathcal{G}_{xx}}{\mathcal{G}} \right) \mathcal{G}_x - \mathcal{r}\mathcal{G}_{xxx} = 0. \quad (1.4)$$

An integrable system acquires the stochasticity when the random or probabilistic elements affect its dynamics. This can occur from the system having random components such as a stochastic differential equation (SDE), Brownian motion, or other causes. The analysis of the stochastic integrable system is inspired by the demand to analyze and understand physical systems that contain both stochastic and deterministic aspects. This approach is particularly useful in areas where the interaction of deterministic laws with random oscillation is essential to the process under investigation such as quantum mechanics. Many researchers have employed a stochastic technique to examine the soliton of integrable systems, see [32–35]. Encouraged by proceeding studies, we seek to explore the Eq (1.4) using a stochastic approach. The SIdV model (1.4) can be reconsidered in stochastic form as

$$\mathcal{G}_t + \left( 3(1 - \varrho)\mathcal{G} + (1 + \varrho)\frac{\mathcal{G}_{xx}}{\mathcal{G}} \right) \mathcal{G}_x - \mathcal{r}\mathcal{G}_{xxx} = \varepsilon \frac{d\mathfrak{W}(t)}{dt}. \quad (1.5)$$

In the above equation, the  $\mathfrak{W}(t)$  denotes the Wiener process (WP), where  $\frac{d\mathfrak{W}(t)}{dt}$  shows white noise. One can obtain the Eq (1.4) when considering  $\varepsilon = 0$  in the Eq (1.5). **(I)** The WP  $\mathfrak{W}(t)$  for  $t \geq 0$  has the following characteristics:

- 1)  $\mathfrak{W}(t) = 0$ , for  $t = 0$ .
- 2)  $\mathfrak{W}(t_i) - \mathfrak{W}(t_j)$ , for  $t_i < t_j$  is independent.
- 3)  $\mathfrak{W}(t)$ ,  $t \geq 0$  is a continuous function for  $t$ .
- 4)  $\mathfrak{W}(t_j) - \mathfrak{W}(t_i)$  has a Gaussian distribution having variance  $t_j - t_i$  and mean 0.

**(II)** The time derivative of a Wiener process, known as white noise, serves as a mathematical abstraction representing phenomena characterized by significant and abrupt fluctuations.

To get analytic solutions for nonlinear PDEs, several methods have been devised. They consist of the extended tanh function method [36], Darboux transformation [37], the Sardar-subequation method [38], and additional ways [39–41]. Three analytical techniques are used in this study: the sine-cosine approach, the modified Kudryashov Technique (KT), and the generalised Kudryashov Technique (KT). These techniques are applied to explore novel analytic solutions for the given model in the stochastic scenario. As far as we know from the literature, this model has not been studied with the proposed methods in the stochastic perspective.

## 2. Generalized Kudryashov method

The significance and practicality of the generalized Kudryashov (GK) method are evident in its ability to pinpoint analytical soliton solutions for nonlinear partial PDEs. In this section, we elucidate the overall procedure of the GK technique to acquire a spectrum of precise solutions for the given model. The GK technique is applied to establish the general form of the solution for the following nonlinear PDE:

$$\mathcal{P}(C, C_x, C_t, C_{xx}, C_{xt}, \dots) = 0, \quad (2.1)$$

where  $C = C(x, t)$ . Consider the transformation presented below

$$\xi = \varpi x - \beta t. \quad (2.2)$$

Now, putting Eq (2.2) into the Eq (2.1), the following ODE can be obtained:

$$\mathcal{G}(C, C', C'', C''', \dots) = 0, \quad (2.3)$$

where “'” denotes ordinary derivatives with respect to  $\xi$ . Subsequently, adopt the provided format for the solution of Eq (2.3), we have

$$\mathcal{G}(x, t) = \frac{Q_0 + \sum_{\gamma=1}^{\varsigma} Q_{\gamma} \mathcal{R}^{\gamma}(\xi)}{\varrho_0 + \sum_{\gamma=1}^{\sigma} \varrho_{\gamma} \mathcal{R}^{\gamma}(\xi)}, \quad (2.4)$$

here,  $\varsigma$  and  $\sigma$  are positive integers, and the coefficients  $Q_{\gamma}$  and  $\varrho_{\gamma}$  (where  $\gamma$  takes values from 1 to  $\varsigma$  and from 1 to  $\sigma$ ) are unspecified and will be determined subsequently. Further  $\xi$  is defined in Eq (2.2). Additionally,

$$\mathcal{R}(\xi) = \frac{1}{1 + \mathcal{A} \exp(\xi)}, \quad (2.5)$$

here  $\mathcal{A}$  denotes constant of integration and  $\mathcal{R}(\xi)$  satisfies the Riccati equation, which is given below:

$$\mathcal{R}'(\xi) = \mathcal{R}^2(\xi) - \mathcal{R}(\xi), \quad (2.6)$$

In this context, the symbol “'” denotes an ordinary derivative w.r.t  $\xi$ . By applying the homogeneous balance law,  $\varsigma$  and  $\sigma$  may be found by comparing the major terms involving the nonlinear term and the highest-order derivative in the resultant ODE, which is generated from several integrations of Eq (2.3). Subsequently, inserting the solutions given by (2.4) and Eq (2.5) into the resulting ODE yields a polynomial in different exponents of  $\mathcal{R}(\xi)$ . Additionally, by setting the powers of  $\mathcal{R}(\xi)$  to zero and equating them, an algebraic system emerges. Evaluating the obtained system allows for the determination of the values of  $Q_\gamma$ ,  $\varrho_\gamma$ , and other parameters, facilitating the finding of solitary waves solution.

### 3. Modified Kudryashov method

Here, the general strategy for the modified KT method is explained. The first step involves identifying an ODE given by Eq (2.3). Subsequently, the expansion that follows can be used:

$$\mathcal{G}(\xi) = \sum_{\kappa=0}^{\vartheta} \frac{\mathcal{F}_\kappa}{(1 + \exp(\xi))^\kappa}, \quad (3.1)$$

where  $\mathcal{F}_0, \mathcal{F}_1, \mathcal{F}_2, \dots, \mathcal{F}_\vartheta$  provide constants which can be obtained from Eq (2.3). The values of  $\vartheta$  may be found by applying the homogeneous balancing principle to the ODE that is produced by repeatedly integrating Eq (2.3). The resultant ODE may be solved by replacing Eq (3.1) and establishing a polynomial in various powers of  $\exp(\xi)$ . An algebraic system results from putting the coefficients of these exponents of  $\exp(\xi)$  to zero. The results for  $\mathcal{F}_\kappa$  and other parameters are obtained by analyzing this system, which makes it easier to derive analytic solutions.

### 4. Applications of the proposed methods

Several novel soliton solutions are computed in this part by applying the suggested approaches to the provided model. Using the following transformation, we start here in order to accomplish this:

$$\mathcal{G}(x, t) = \mathcal{V}(\xi) = (\varpi x - \beta t) e^{\varepsilon \mathbb{B}(t) - \varepsilon^2 \frac{t^2}{2}}, \quad \xi = \varpi x - \beta t. \quad (4.1)$$

On inserting the Eq (4.1) into Eq (1.5), following ODE can be obtained

$$\mathcal{V}(\xi) \left( -\varpi^3 - \gamma \mathcal{V}(\xi)^3 - \beta \mathcal{V}'(\xi) + \varpi \mathcal{V}'(\xi) \left( \frac{\varpi^2 (\varrho + 1) \mathcal{V}''(\xi)}{\mathcal{V}(\xi)} + 3(1 - \varrho) \mathcal{V}(\xi) \right) \right) = 0. \quad (4.2)$$

Integrating Eq (4.2) and considering integration constant as zero we get:

$$-2\varpi^3 \gamma \mathcal{V}(\xi) \mathcal{V}''(\xi) + \varpi^3 (\gamma + \varrho + 1) \mathcal{V}'(\xi)^2 - \beta \mathcal{V}(\xi)^2 - 2\varpi(\varrho - 1) \mathcal{V}(\xi)^3 = 0. \quad (4.3)$$

By the homogenous balancing rule, we can articulate:

$$\varsigma = \sigma + 2, \quad (4.4)$$

where  $\sigma \neq 0$ .

#### 4.1. Solutions with GK method

To study implications of the GK technique, considering Eq (4.4) with  $\sigma = 1$ , it follows from Eq (4.4) that  $\zeta = 3$ . Consequently, the general solution of the Eq (4.3) takes the form:

$$\mathcal{G}(x, t) = \mathcal{V}(\xi) = \frac{\mathcal{Q}_0 + \mathcal{Q}_1\mathcal{R}(\xi) + \mathcal{Q}_2\mathcal{R}^2(\xi) + \mathcal{Q}_3\mathcal{R}^3(\xi)}{\zeta_0 + \zeta_1\mathcal{R}(\xi)}. \quad (4.5)$$

Inserting Eq (4.5) into the Eq (4.3), we get

$$\begin{aligned} & -2\varpi^3\mathcal{Y}(\mathcal{R}(\xi) - 1)\mathcal{R}(\xi)\mathcal{R}(\xi)^2(\mathcal{Q}_2 + \mathcal{Q}_3) + \mathcal{Q}_1 + \mathcal{Q}_0) (\mathcal{R}(\xi)) (\mathcal{R}(\xi))(\mathcal{Q}_2 + \mathcal{Q}_3)(\zeta_1\mathcal{R}(\xi))(2\zeta_1\mathcal{R}(\xi)) \\ & + 6\zeta_0 - \zeta_1) + 3\zeta_0(2\zeta_0 - \zeta_1)) + \zeta_0\zeta_1(\mathcal{Q}_1 - 2\mathcal{Q}_0) - \mathcal{Q}_0\zeta_1^2 + 2\zeta_0^2(\mathcal{Q}_1 - 2(\mathcal{Q}_2 + \mathcal{Q}_3)) + \zeta_0(\mathcal{Q}_0\zeta_1 - \mathcal{Q}_1\zeta_0)) \\ & + \varpi^3(\mathcal{R}(\xi) - 1)^2\mathcal{R}(\xi)^2(\mathcal{Y} + \varrho + 1)(\mathcal{R}(\xi))(\mathcal{Q}_2 + \mathcal{Q}_3)(\zeta_1\mathcal{R}(\xi)) + 2\zeta_0) - \mathcal{Q}_0\zeta_1 + \mathcal{Q}_1\zeta_0)^2 \\ & - 2\varpi(\varrho - 1)(\zeta_1\mathcal{R}(\xi) + \zeta_0) \times \mathcal{R}(\xi)^2(\mathcal{Q}_2 + \mathcal{Q}_3) + \mathcal{Q}_1 + \mathcal{Q}_0)^3 - \beta(\zeta_1\mathcal{R}(\xi) + \zeta_0)^2\mathcal{R}(\xi)^2 \\ & \times (\mathcal{Q}_2 + \mathcal{Q}_3) + \mathcal{Q}_1 + \mathcal{Q}_0)^2 = 0. \end{aligned} \quad (4.6)$$

By comparing various powers of  $\mathcal{R}(\xi)$ , we derived a system of algebraic equations, the solution of which yields the following values for the unknown parameters:

$$\begin{aligned} \text{Set I : } & \mathcal{Q}_0 = -\frac{\varpi^2\mathcal{Y}\zeta_0}{\varrho - 1}, \mathcal{Q}_2 = -\mathcal{Q}_3, \zeta_1 = \frac{\mathcal{Q}_1 - \varrho\mathcal{Q}_1}{\varpi^2\mathcal{Y}}, \beta = 2\varpi^3\mathcal{Y} \\ \text{Set II : } & \mathcal{Q}_0 = -\frac{\varpi^2\mathcal{Y}\zeta_0}{\varrho - 1}, \mathcal{Q}_1 = \frac{\varpi^2\mathcal{Y}\zeta_0}{\varrho - 1}, \mathcal{Q}_2 = -\mathcal{Q}_3, \zeta_1 = -\zeta_0, \beta = 2\varpi^3\mathcal{Y} \\ \text{Set III : } & \mathcal{Q}_0 = 0, \mathcal{Q}_1 = -\frac{2\varpi^2\zeta_0(\varrho - 2\mathcal{Y} + 1)}{\varrho - 1}, \mathcal{Q}_2 = \frac{2\varrho\varpi^2\zeta_0 - 4\varpi^2\mathcal{Y}\zeta_0 + 2\varpi^2\zeta_0 - \varrho\mathcal{Q}_3 + \mathcal{Q}_3}{\varrho - 1}, \\ & \zeta_1 = 0, \beta = \varpi^3(-\mathcal{Y} + 1 + \varrho). \end{aligned}$$

Inserting the aforementioned sets of parameters into Eq (4.5) and utilizing Eq (4.1), one derive:

$$S_1 = e^{\varepsilon\mathbb{B}(t) - \varepsilon^2\frac{t^2}{2}} \left( \frac{\frac{\mathcal{Q}_3}{(\mathcal{A}e^{\varpi x - 2\varpi^3\mathcal{Y}t + 1})^3} - \frac{\mathcal{Q}_3}{(\mathcal{A}e^{\varpi x - 2\varpi^3\mathcal{Y}t + 1})^2} - \frac{\varpi^2\mathcal{Y}\zeta_0}{\varrho - 1} + \frac{\varpi^2\mathcal{Y}\zeta_0}{(\varrho - 1)(\mathcal{A}e^{\varpi x - 2\varpi^3\mathcal{Y}t + 1})}}{\zeta_0 - \frac{\zeta_0}{\mathcal{A}e^{\varpi x - 2\varpi^3\mathcal{Y}t + 1}}} \right). \quad (4.7)$$

$$S_2 = e^{\varepsilon\mathbb{B}(t) - \varepsilon^2\frac{t^2}{2}} \left( \frac{\frac{\varpi^2\mathcal{Y}\zeta_0}{(\varrho - 1)(\mathcal{A}e^{\varpi x - \beta t + 1})} - \frac{\varpi^2\mathcal{Y}\zeta_0}{\varrho - 1} - \frac{\mathcal{Q}_3}{(\mathcal{A}e^{\varpi x - \beta t + 1})^2} + \frac{\mathcal{Q}_3}{(\mathcal{A}e^{\varpi x - \beta t + 1})^3}}{\zeta_0 - \frac{\zeta_0}{\mathcal{A}e^{\varpi x - \beta t + 1}}} \right). \quad (4.8)$$

$$S_3 = e^{\varepsilon\mathbb{B}(t) - \varepsilon^2\frac{t^2}{2}} \left( \frac{\frac{\mathcal{Q}_3}{(\mathcal{A}e^{\varpi x - \varpi^3 t(\varrho - \mathcal{Y} + 1) + 1})^3} + \frac{2\varrho\varpi^2\zeta_0 - 4\varpi^2\mathcal{Y}\zeta_0 + 2\varpi^2\zeta_0 - \varrho\mathcal{Q}_3 + \mathcal{Q}_3}{(\varrho - 1)(\mathcal{A}e^{\varpi x - \varpi^3 t(\varrho - \mathcal{Y} + 1) + 1})^2} - \frac{2\varpi^2\zeta_0(\varrho - 2\mathcal{Y} + 1)}{(\varrho - 1)(\mathcal{A}e^{\varpi x - \varpi^3 t(\varrho - \mathcal{Y} + 1) + 1})}}{\zeta_0} \right). \quad (4.9)$$

#### 4.2. Solutions with MK method

In this section, we demonstrate the implication of the MK method. By employing the homogeneous balance principle on Eq (3.1), we determine that  $\vartheta = 2$ . Consequently, using Eq (3.1), one obtain:

$$\mathcal{G}(x, t) = \mathcal{V}(\xi) = \mathcal{F}_0 + \frac{\mathcal{F}_1}{1 + \exp(\xi)} + \frac{\mathcal{F}_2}{(1 + \exp(\xi))^2}. \quad (4.10)$$

By substituting Eq (4.10) into Eq (4.2), we derive the following:

$$\begin{aligned} & -2\omega^3 \Upsilon e^{\omega x + \beta t} \left( \mathcal{F}_1 (e^{2\omega x + \beta t} - 1) + 2\mathcal{F}_2 (2e^{\omega x + \beta t} - 1) \right) \left( \mathcal{F}_0 (e^{\omega x + \beta t} + 1)^2 + \mathcal{F}_1 e^{\omega x + \beta t} + \mathcal{F}_1 + \mathcal{F}_2 \right) \\ & + 2(1 - \varrho) \omega \left( \mathcal{F}_0 (e^{\omega x + \beta t} + 1)^2 + \mathcal{F}_1 e^{\omega x + \beta t} + \mathcal{F}_1 + \mathcal{F}_2 \right)^3 - (e^{\omega x + \beta t} + 1)^2 \varrho \left( \mathcal{F}_0 (e^{\omega x + \beta t} + 1)^2 \right. \\ & \left. + \mathcal{F}_1 e^{\omega x + \beta t} + \mathcal{F}_1 + \mathcal{F}_2 \right)^2 + \omega^3 e^{2\omega x + \beta t} (\beta + \Upsilon + 1) \left( \mathcal{F}_1 e^{\omega x + \beta t} + \mathcal{F}_1 + 2\mathcal{F}_2 \right)^2 = 0. \end{aligned} \quad (4.11)$$

Comparing various powers of  $\exp(\xi)$ ,  $\xi = 2\omega x + \beta t$ , we get

$$\begin{aligned} (e^\xi)^0 : & -2\varrho \mathcal{F}_0^3 \omega + 2\mathcal{F}_0^3 \omega - 6\varrho \mathcal{F}_0^2 \mathcal{F}_1 \omega + 6\mathcal{F}_0^2 \mathcal{F}_1 \omega - 6\varrho \mathcal{F}_0^2 \mathcal{F}_2 \omega + 6\mathcal{F}_0^2 \mathcal{F}_2 \omega - \mathcal{F}_0^2 \beta - 6\varrho \mathcal{F}_0 \mathcal{F}_1^2 \omega \\ & - 12\varrho \mathcal{F}_0 \mathcal{F}_1 \mathcal{F}_2 \omega + 12\mathcal{F}_0 \mathcal{F}_1 \mathcal{F}_2 \omega - 2\mathcal{F}_0 \mathcal{F}_1 \beta - 6\varrho \mathcal{F}_0 \mathcal{F}_2^2 \omega + 6\mathcal{F}_0 \mathcal{F}_2^2 \omega - 2\mathcal{F}_0 \mathcal{F}_2 \beta - 2\varrho \mathcal{F}_1^3 \omega + 2\mathcal{F}_1^3 \omega \\ & - 6\varrho \mathcal{F}_1^2 \mathcal{F}_2 \omega + 6\mathcal{F}_1^2 \mathcal{F}_2 \omega - \mathcal{F}_1^2 \beta - 6\varrho \mathcal{F}_1 \mathcal{F}_2^2 \omega + 6\mathcal{F}_1 \mathcal{F}_2^2 \omega - 2\mathcal{F}_1 \mathcal{F}_2 \beta - 2\varrho \mathcal{F}_2^3 \omega + 2\mathcal{F}_2^3 \omega - \mathcal{F}_2^2 \beta \\ & + 6\mathcal{F}_0 \mathcal{F}_1^2 \omega = 0 \\ (e^\xi)^1 : & -2\varrho \mathcal{F}_0^3 \omega + 2\mathcal{F}_0^3 \omega - \mathcal{F}_0^2 \beta = 0 \\ (e^\xi)^2 : & -12\varrho \mathcal{F}_0^3 \omega + 12\mathcal{F}_0^3 \omega - 6\varrho \mathcal{F}_0^2 \mathcal{F}_1 \omega + 6\mathcal{F}_0^2 \mathcal{F}_1 \omega - 6\mathcal{F}_0^2 \beta - 2\mathcal{F}_0 \mathcal{F}_1 \omega^3 \Upsilon - 2\mathcal{F}_0 \mathcal{F}_1 \beta = 0 \\ (e^\xi)^3 : & -30\varrho \mathcal{F}_0^3 \omega + 30\mathcal{F}_0^3 \omega - 30\varrho \mathcal{F}_0^2 \mathcal{F}_1 \omega + 30\mathcal{F}_0^2 \mathcal{F}_1 \omega - 6\varrho \mathcal{F}_0^2 \mathcal{F}_2 \omega + 6\mathcal{F}_0^2 \mathcal{F}_2 \omega - 15\mathcal{F}_0^2 \beta \\ & + 6\mathcal{F}_0 \mathcal{F}_1^2 \omega - 4\mathcal{F}_0 \mathcal{F}_1 \omega^3 \Upsilon - 10\mathcal{F}_0 \mathcal{F}_1 \beta - 8\mathcal{F}_0 \mathcal{F}_2 \omega^3 \Upsilon - 2\mathcal{F}_0 \mathcal{F}_2 \beta + \varrho \mathcal{F}_1^2 \omega^3 - \mathcal{F}_1^2 \omega^3 \Upsilon + \mathcal{F}_1^2 \omega^3 \\ & - \mathcal{F}_1^2 \beta - 6\varrho \mathcal{F}_0 \mathcal{F}_1^2 \omega = 0 \\ (e^\xi)^4 : & -40\varrho \mathcal{F}_0^3 \omega + 40\mathcal{F}_0^3 \omega - 60\varrho \mathcal{F}_0^2 \mathcal{F}_1 \omega + 60\mathcal{F}_0^2 \mathcal{F}_1 \omega - 24\varrho \mathcal{F}_0^2 \mathcal{F}_2 \omega + 24\mathcal{F}_0^2 \mathcal{F}_2 \omega \\ & + 24\mathcal{F}_0 \mathcal{F}_1^2 \omega - 12\varrho \mathcal{F}_0 \mathcal{F}_1 \mathcal{F}_2 \omega + 12\mathcal{F}_0 \mathcal{F}_1 \mathcal{F}_2 \omega - 20\mathcal{F}_0 \mathcal{F}_1 \beta - 12\mathcal{F}_0 \mathcal{F}_2 \omega^3 \Upsilon - 8\mathcal{F}_0 \mathcal{F}_2 \beta - 2\varrho \mathcal{F}_1^3 \omega \\ & + 2\varrho \mathcal{F}_1^2 \omega^3 + 2\mathcal{F}_1^2 \omega^3 - 4\mathcal{F}_1^2 \beta + 4\varrho \mathcal{F}_1 \mathcal{F}_2 \omega^3 - 6\mathcal{F}_1 \mathcal{F}_2 \omega^3 \Upsilon + 4\mathcal{F}_1 \mathcal{F}_2 \omega^3 - 2\mathcal{F}_1 \mathcal{F}_2 \beta - 20\mathcal{F}_0^2 \beta \\ & - 24\varrho \mathcal{F}_0 \mathcal{F}_1^2 \omega + 2\mathcal{F}_1^3 \omega = 0 \\ \exp(\xi)^5 : & -12\varrho \mathcal{F}_0^3 \omega + 12\mathcal{F}_0^3 \omega - 30\varrho \mathcal{F}_0^2 \mathcal{F}_1 \omega + 30\mathcal{F}_0^2 \mathcal{F}_1 \omega - 24\varrho \mathcal{F}_0^2 \mathcal{F}_2 \omega + 24\mathcal{F}_0^2 \mathcal{F}_2 \omega - 6\mathcal{F}_0^2 \beta \\ & + 24\mathcal{F}_0 \mathcal{F}_1^2 \omega - 36\varrho \mathcal{F}_0 \mathcal{F}_1 \mathcal{F}_2 \omega + 36\mathcal{F}_0 \mathcal{F}_1 \mathcal{F}_2 \omega + 2\mathcal{F}_0 \mathcal{F}_1 \omega^3 \Upsilon - 10\mathcal{F}_0 \mathcal{F}_1 \beta - 12\varrho \mathcal{F}_0 \mathcal{F}_2^2 \omega + 12\mathcal{F}_0 \mathcal{F}_2^2 \omega \\ & + 4\mathcal{F}_0 \mathcal{F}_2 \omega^3 \Upsilon - 8\mathcal{F}_0 \mathcal{F}_2 \beta - 6\varrho \mathcal{F}_1^3 \omega + 6\mathcal{F}_1^3 \omega - 12\varrho \mathcal{F}_1^2 \mathcal{F}_2 \omega + 12\mathcal{F}_1^2 \mathcal{F}_2 \omega + 2\mathcal{F}_1^2 \omega^3 \Upsilon - 4\mathcal{F}_1^2 \beta \\ & - 6\varrho \mathcal{F}_1 \mathcal{F}_2^2 \omega + 6\mathcal{F}_1 \mathcal{F}_2^2 \omega + 6\mathcal{F}_1 \mathcal{F}_2 \omega^3 \Upsilon - 6\mathcal{F}_1 \mathcal{F}_2 \beta + 4\mathcal{F}_2^2 \omega^3 \Upsilon - 2\mathcal{F}_2^2 \beta - 24\varrho \mathcal{F}_0 \mathcal{F}_1^2 \omega = 0 \\ (e^\xi)^6 : & -30\varrho \mathcal{F}_0^3 \omega + 30\mathcal{F}_0^3 \omega - 60\varrho \mathcal{F}_0^2 \mathcal{F}_1 \omega + 60\mathcal{F}_0^2 \mathcal{F}_1 \omega - 36\varrho \mathcal{F}_0^2 \mathcal{F}_2 \omega + 36\mathcal{F}_0^2 \mathcal{F}_2 \omega - 15\mathcal{F}_0^2 \beta \\ & + 36\mathcal{F}_0 \mathcal{F}_1^2 \omega - 36\varrho \mathcal{F}_0 \mathcal{F}_1 \mathcal{F}_2 \omega + 36\mathcal{F}_0 \mathcal{F}_1 \mathcal{F}_2 \omega + 4\mathcal{F}_0 \mathcal{F}_1 \omega^3 \Upsilon - 20\mathcal{F}_0 \mathcal{F}_1 \beta - 6\varrho \mathcal{F}_0 \mathcal{F}_2^2 \omega + 6\mathcal{F}_0 \mathcal{F}_2^2 \omega \\ & - 12\mathcal{F}_0 \mathcal{F}_2 \beta - 6\varrho \mathcal{F}_1^3 \omega + 6\mathcal{F}_1^3 \omega - 6\varrho \mathcal{F}_1^2 \mathcal{F}_2 \omega + 6\mathcal{F}_1^2 \mathcal{F}_2 \omega + \varrho \mathcal{F}_1^2 \omega^3 + 3\mathcal{F}_1^2 \omega^3 \Upsilon + \mathcal{F}_1^2 \omega^3 - 6\mathcal{F}_1^2 \beta \\ & + 4\varrho \mathcal{F}_1 \mathcal{F}_2 \omega^3 + 4\mathcal{F}_1 \mathcal{F}_2 \omega^3 - 6\mathcal{F}_1 \mathcal{F}_2 \beta + 4\varrho \mathcal{F}_2^2 \omega^3 - 4\mathcal{F}_2^2 \omega^3 \Upsilon + 4\mathcal{F}_2^2 \omega^3 - \mathcal{F}_2^2 \beta - 36\varrho \mathcal{F}_0 \mathcal{F}_1^2 \omega = 0. \end{aligned} \quad (4.12)$$

Upon solving the aforementioned system, we acquire:

$$\mathcal{F}_0 = 0, \mathcal{F}_1 = -\frac{2\omega^2(\varrho - 2\Upsilon + 1)}{\varrho - 1}, \mathcal{F}_2 = \frac{2(\varrho\omega^2 - 2\omega^2\Upsilon + \omega^2)}{\varrho - 1}, \beta = \omega^3(\varrho - \Upsilon + 1), \quad (4.13)$$

Putting the values presented above in Eq (4.10), we obtained the following solution

$$S_4 = e^{\varepsilon \mathbb{B}(t) - \varepsilon^2 \frac{t^2}{2}} \left( \frac{2(\varrho \varpi^2 - 2\varpi^2 \Upsilon + \varpi^2)}{(\varrho - 1)(e^{\varpi x - \varpi^3 t(\varrho - \Upsilon + 1)} + 1)^2} - \frac{2\varpi^2(\varrho - 2\Upsilon + 1)}{(\varrho - 1)(e^{\varpi x - \varpi^3 t(\varrho - \Upsilon + 1)} + 1)} \right). \quad (4.14)$$

### 4.3. Solutions with sine-cosine procedure

Here, the sine-cosine method to compute more closed form solutions for the proposed stochastic nonlinear equation is presented. This method involves utilizing the sine expansion give as:

$$\mathcal{G}(x, t) = \mathcal{V}(\xi) = \Omega \sin(\mu \xi)^r, \quad (4.15)$$

where

$$\mathcal{V}(\xi)'' = r(r-1)\Omega\mu^2 \sin(\mu\xi)^{r-2} - r^2\Omega\mu^2 \sin(\mu\xi)^r. \quad (4.16)$$

Inserting Eq (4.15) and the Eq (4.16) into Eq (4.2), we get

$$\begin{aligned} & -\Omega^2\beta(\sin(\mu\xi))^{2r} - 2\varpi(-1+\beta)\Omega^3(\sin(\mu\xi))^{3r} + (\varpi)^3r^2(1+\beta+\Upsilon)\Omega^2(\mu)^2 \\ & (1 - (\sin(\mu\xi))^2)(\sin(\mu\xi))^{-2+2r} - 2\varpi^3\Upsilon\Omega(\sin(\mu\xi))^r((-1+r)r\Omega\mu^2 \\ & (1 - (\sin(\mu\xi))^2)(\sin(\mu\xi))^{-2+r} - r\Omega(\mu)^2(\sin(\mu\xi))^r) = 0. \end{aligned} \quad (4.17)$$

One reach to:

$$\begin{aligned} r - 2 & \neq 0 \\ 3r + 2 - 2r & = 0 \\ \beta r^2 \varpi^3 \Omega^2 \mu^2 - r^2 \varpi^3 \Upsilon \Omega^2 \mu^2 + r^2 \varpi^3 \Omega^2 \mu^2 + 2r \varpi^3 \Upsilon \Omega^2 \mu^2 - 2\varrho \varpi \Omega^3 + 2\varpi \Omega^3 & = 0 \\ -\varrho r^2 \varpi^3 \Omega^2 \mu^2 + r^2 \varpi^3 \Upsilon \Omega^2 \mu^2 - \varpi^3 r^2 \Omega^2 \mu^2 - \Omega^2 \nu & = 0. \end{aligned} \quad (4.18)$$

Solving system (4.18), we get the following

$$\begin{aligned} r = -2, \mu & = -\frac{\sqrt{\mu}}{2\sqrt{-\varrho\varpi^3 + \varpi^3\Upsilon - \varpi^3}}, \Omega = \frac{-\varrho\mu + 2\Upsilon\mu - \mu}{2(-1 + \varrho)\varpi(-\Upsilon + \varrho + 1)}, \\ r = -2, \mu & = \frac{\sqrt{\mu}}{2\sqrt{-\varrho\varpi^3 + \varpi^3\Upsilon - \varpi^3}}, \Omega = \frac{-\varrho\mu + 2\Upsilon\mu - \mu}{2(-1 + \varrho)\varpi(-\Upsilon + \varrho + 1)}. \end{aligned} \quad (4.19)$$

By substituting the aforementioned values into Eq (4.15), we reach:

$$S_5 = e^{\varepsilon \mathbb{B}(t) - \varepsilon^2 \frac{t^2}{2}} \left( \frac{(-\varrho\mu + 2\Upsilon\mu - \mu) \csc^2 \left( \frac{\sqrt{\mu}(\varpi x - \beta t)}{2\sqrt{-\varrho\varpi^3 + \varpi^3\Upsilon - \varpi^3}} \right)}{2(-1 + \varrho)\varpi(-\Upsilon + \varrho + 1)} \right). \quad (4.20)$$

$$S_6 = e^{\varepsilon \mathbb{B}(t) - \varepsilon^2 \frac{t^2}{2}} \left( \frac{(-\varrho\mu + 2\Upsilon\mu - \mu) \csc^2 \left( \frac{\sqrt{\mu}(\varpi x - \beta t)}{2\sqrt{-\varrho\varpi^3 + \varpi^3\Upsilon - \varpi^3}} \right)}{2(-1 + \varrho)\varpi(-\Upsilon + \varrho + 1)} \right). \quad (4.21)$$



Next suppose the Cosine expansion:

$$\mathcal{G}(x, t) = \mathcal{V}(\xi) = \Omega \cos(\mu\xi)^r, \quad (4.22)$$

here

$$\mathcal{V}(\xi)'' = r(r-1)\Omega\mu^2 \cos(\mu\xi)^{r-2} - r^2\Omega\mu^2 \cos(\mu\xi)^r. \quad (4.23)$$

Inserting Eq (4.22) and the Eq (4.23) into Eq (4.2), we get

$$\begin{aligned} & -\Omega^2\beta(\cos(\mu\xi))^{2r} - 2\varpi(-1+\beta)\Omega^3(\cos(\mu\xi))^{3r} + \varpi^3r^2(1+\beta+\Upsilon)\Omega^2\mu^2 \\ & (1 - (\cos(\mu\xi))^2)(\cos(\mu\xi))^{-2+2r} - 2\varpi^3\Upsilon\Omega(\cos(\mu\xi))^r((-1+r)r\Omega\mu^2 \\ & (1 - (\cos(\mu\xi))^2)(\cos(\mu\xi))^{-2+r} - r\Omega\mu^2(\cos(\mu\xi))^r) = 0. \end{aligned} \quad (4.24)$$

One scenario that may occur is as:

$$\begin{aligned} r-2 & \neq 0 \\ 3r+2-2r & = 0 \\ \beta r^2\varpi^3\Omega^2\mu^2 - r^2\varpi^3\Upsilon\Omega^2\mu^2 + r^2\varpi^3\Omega^2\mu^2 + 2r\varpi^3\Upsilon\Omega^2\mu^2 - 2\varrho\varpi\Omega^3 + 2\varpi\Omega^3 & = 0 \\ -\varrho r^2\varpi^3\Omega^2\mu^2 + r^2\varpi^3\Upsilon\Omega^2\mu^2 - \varpi^3r^2\Omega^2\mu^2 - \Omega^2\nu & = 0. \end{aligned} \quad (4.25)$$

The values obtained by solving the given system are:

$$\begin{aligned} r = -2, \mu & = -\frac{\sqrt{\mu}}{2\sqrt{-\varrho\varpi^3 + \varpi^3\Upsilon - \varpi^3}}, \Omega = \frac{-\varrho\mu + 2\Upsilon\mu - \mu}{2(-1+\varrho)\varpi(-\Upsilon + \varrho + 1)}, \\ r = -2, \mu & = \frac{\sqrt{\mu}}{2\sqrt{-\varrho\varpi^3 + \varpi^3\Upsilon - \varpi^3}}, \Omega = \frac{-\varrho\mu + 2\Upsilon\mu - \mu}{2(-1+\varrho)\varpi(-\Upsilon + \varrho + 1)}. \end{aligned} \quad (4.26)$$

We obtain the following solutions by entering the aforementioned values into Eq (4.22).

$$S_7 = e^{\varepsilon\mathfrak{B}(t) - \varepsilon^2\frac{t^2}{2}} \left( \frac{(-\varrho\beta + 2\Upsilon\beta - \beta) \sec^2\left(\frac{\sqrt{\beta}(\varpi x - \beta t)}{2\sqrt{-\varrho\varpi^3 + \varpi^3\Upsilon - \varpi^3}}\right)}{2(-1+\varrho)\varpi(-\Upsilon + \varrho + 1)} \right). \quad (4.27)$$

$$S_8 = e^{\varepsilon\mathfrak{B}(t) - \varepsilon^2\frac{t^2}{2}} \left( \frac{(-\varrho\beta + 2\Upsilon\beta - \beta) \sec^2\left(\frac{\sqrt{\beta}(\varpi x - \beta t)}{2\sqrt{-\varrho\varpi^3 + \varpi^3\Upsilon - \varpi^3}}\right)}{2(-1+\varrho)\varpi(-\Upsilon + \varrho + 1)} \right). \quad (4.28)$$

#### 4.4. Graphical illustrations and discussion

This section provides a detailed analysis of the geometric characteristics of various solutions we have derived. It includes both 2D and 3D visual representations to elucidate their physical implications. Specifically, we examine the shape of solution  $S_1$ , as depicted in Figure 1. Here, the behavior of

the kink solitary wave is presented in both two and three dimensions, characterized by a localized wave profile with a sharply defined amplitude shift. Additionally, Figure 1 contains subfigures that investigate the influence of noise on these observations. We particularly focus on how the kink solitary waves respond to varying levels of  $\omega$ , demonstrating that these waves undergo significant changes. This observation underscores the sensitivity of kink solitary wave dynamics to fluctuations in the  $\omega$  parameter, thereby shedding light on the impact of noise on the dynamic properties of the solutions being studied.

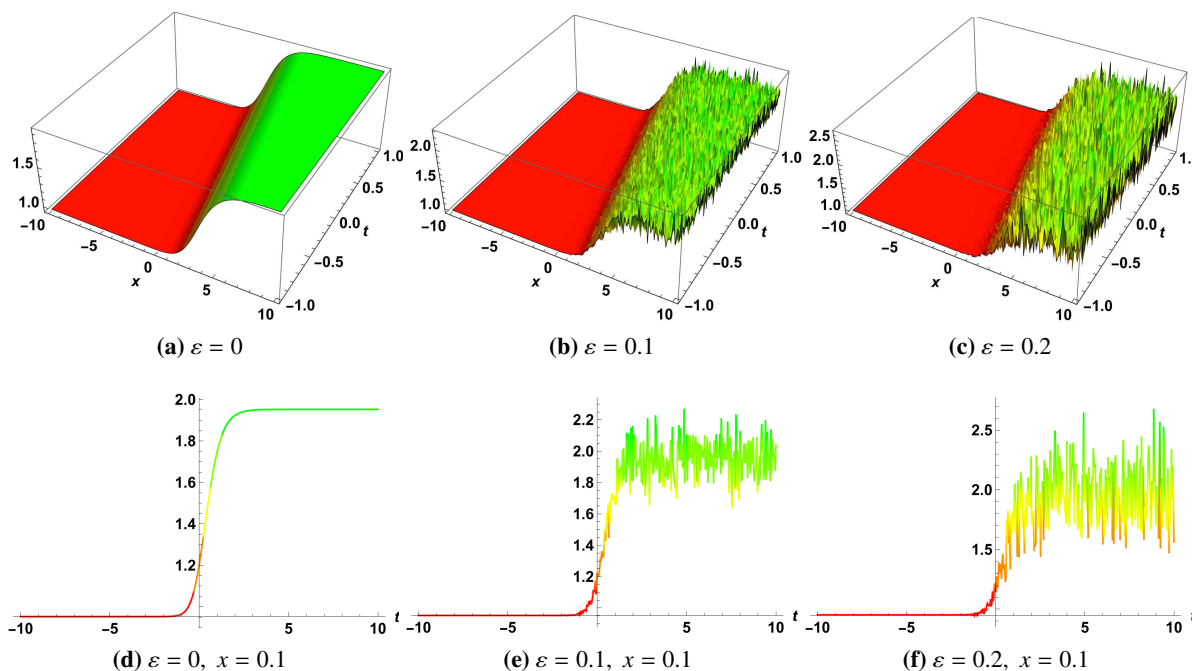


**Figure 1.** Three and two dimensional dynamics of  $S_1$  for  $\gamma = 2$ ,  $\mathcal{A} = 2$ ,  $\varpi = 1$ ,  $Q_3 = 1$ ,  $\zeta_0 = 1$ ,  $\varrho = -1.1$ .

The graphical view of the solution  $S_2$  is presented in Figure 2, revealing periodic solitonic patterns in two- and three-dimensional representations. Solitons are waves that travel alone and maintain their shape and speed. The steady, recurring waveforms in this illustration are known as soliton waveforms. Additionally, a graphic explanation of the noise term's influence is provided. A comparable increase in the periodic soliton's unpredictability is observed when the noise term's amplitude increases. The impact of the noise factor on the formerly stable and periodic solitonic patterns is well depicted in this visual aid, highlighting the system's vulnerability to changes in the noise parameter.

Furthermore, Figure 3 shows the dynamics of the solution  $S_4$  in two- and three-dimensional representations, illustrating a dark soliton configuration typical. The visualization's subfigures illuminate how the noise term affects the dynamics that are intrinsic to the dark soliton structure. In particular, a visual representation of the effect of changing the noise term is provided. There is a discernible impact on the dark soliton's behaviour as the noise term's amplitude increases. This indicates a significant rise in the variation that the dark soliton displays. Essentially, the graphic conveys how sensitive the behavior of the dark soliton is to changes in the noise parameter, offering important information on the complex interactions between the soliton structure and the stochasticity of the environment.

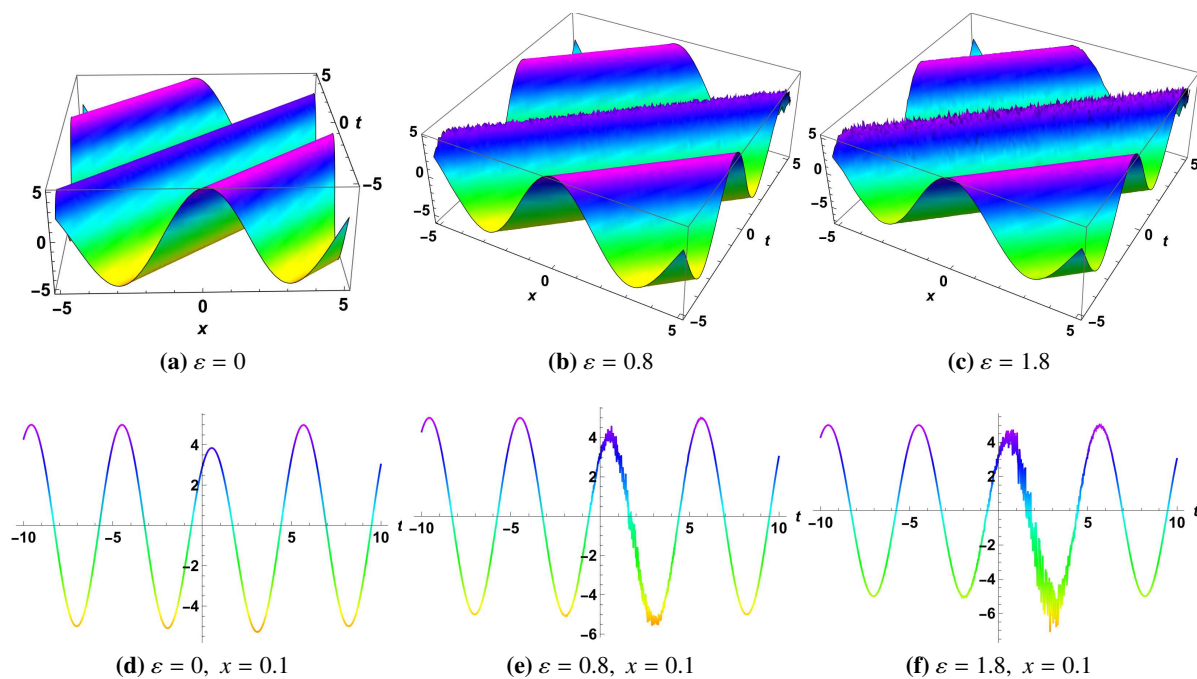


**Figure 2.** Three and two dimensional dynamics of  $S_2$  for  $\gamma = 1, \mathcal{A} = 1, \varpi = 0.1, Q_3 = 1, \zeta_0 = 0.2, \rho = 0.1$ .

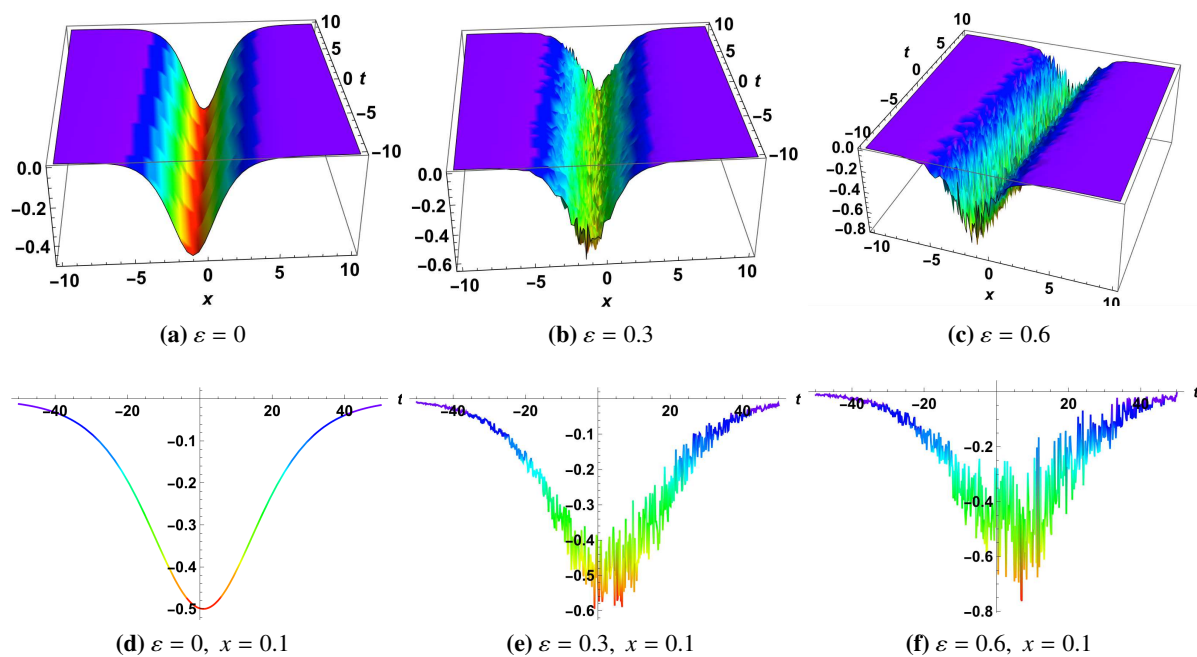


**Figure 3.** Three and two dimensional dynamics of  $S_4$  for  $\rho = 1, \gamma = 1, \varpi = 1$ .

A graphic depiction of the solution  $S_5$  is shown in Figure 4, which depicts a localised wave with sharp peaks and periodicity. Localized wave patterns become crucial in our analysis, as the well-defined, sharp peaks they exhibit signify the presence of a distinct wave packet. The graphical

representation not only offers insights into the periodic behavior and amplitude distribution of these localized waves but also elucidates their dynamic properties. The series culminates with Figure 5, presenting a detailed portrayal of the geometric attributes of solution  $S_6$ . The bell-shaped contour characteristic of this solution distinctly indicates a localized wave. The clearly defined concentration region suggests that the bell-shaped form may mirror specific physical events. The graphical depiction facilitates a better understanding of solution  $S_6$ , which has unique wave profile properties. Additionally, by incorporating noise terms in the subfigures, we explore the impact of unpredictability on the system. Observations from these subfigures reveal that as the value of the noise term increases, the dynamics of the wave behavior fluctuate more intensely. This research underscores how stochastic factors influence localized wave solutions and provides valuable insights into the system's response to heightened ambient noise levels.

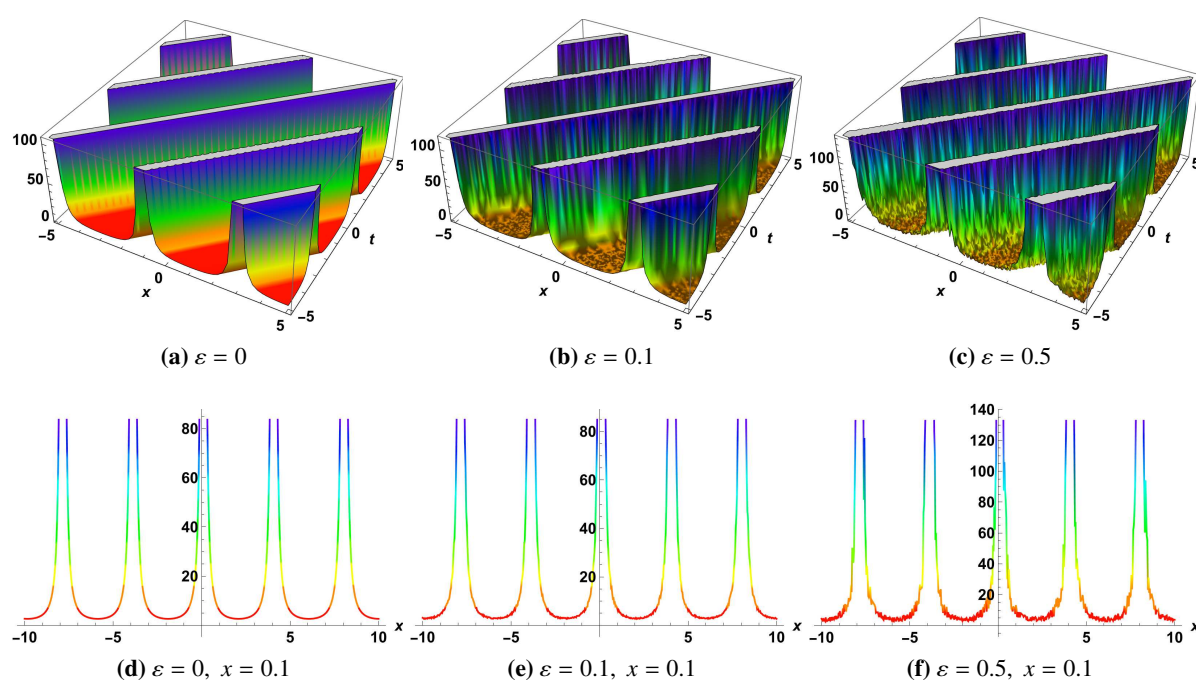


**Figure 4.** Three and two dimensional dynamics of  $S_5$  for  $\varrho = 0.1$ ,  $\gamma = 1.5$ ,  $\beta = 1$ ,  $\varpi = 1$ .

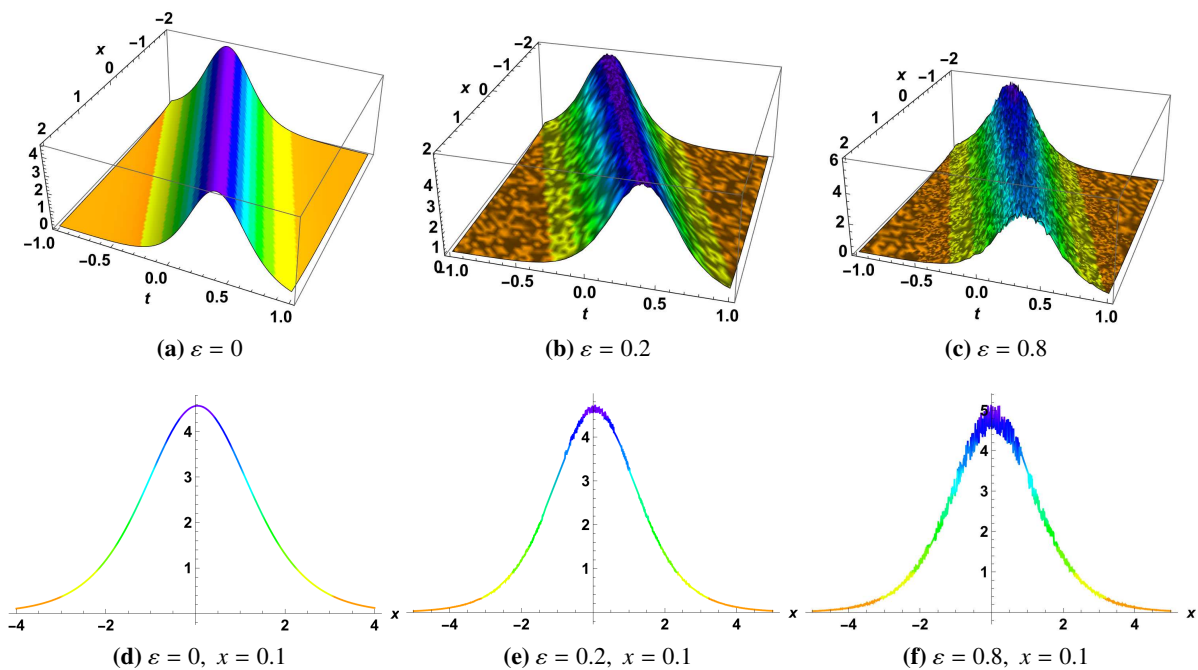


**Figure 5.** Three and two dimensional dynamics of  $S_6$  for  $\varrho = 0.1$ ,  $\gamma = -2$ ,  $\beta = 5$ ,  $\varpi = 1$ .

## 5. Conclusions

In summary, the inherent stochasticity of many physical systems necessitates the use of stochastic methods to effectively seek soliton solutions. Incorporating randomness into our models provides invaluable insights into the impact of uncertainty on soliton dynamics, offering a deeper understanding of their stability and interactions within real-world scenarios. By introducing the Wiener process into the SIdV equation, we aim to capture the realistic behavior of solitons under stochastic influences. Through meticulous analysis utilizing advanced techniques like the generalized KT, its modified counterpart, and the sine-cosine procedure, we unveil a diverse array of traveling wave solutions. These solutions encompass both solitary waves and bounded waveforms, offering a comprehensive view of soliton dynamics. This underscores the significance of stochastic methodologies in unraveling the complexities of physical systems, emphasizing their role in enhancing our comprehension of fundamental phenomena.

Solitons exhibit stable, periodic waveforms unaffected by external influences, while increased noise disrupts their predictability, revealing system vulnerability. Dark solitons, depicted in Figure 3, display sensitivity to noise, with amplified variation in behavior as noise amplitude rises, highlighting complex soliton-environment interactions. Localized wave patterns in Figures 4 and 5 reveal distinct wave packets, with sharp peaks and periodicity, while noise introduction demonstrates heightened fluctuations in wave behavior, emphasizing stochastic influence on localized wave solutions. Furthermore, the diverse physical explanation of acquired solutions highlight the wide-ranging evolution produced by the generalized stochastic SIdV equation. The findings offer new perspectives on wave propagation in stochastic environments, unveiling various phenomena like dark soliton structures, periodic solitonic patterns, and kink-solitary waves. Analyzing and interpreting these geometric characteristics is vital for unraveling the complex relationship between dispersive and

nonlinear effects in various physical contexts. Future work includes analysis of the proposed model where the neural networks will be carried out [42, 43].

### Use of AI tools declaration

The authors declare they have not used Artificial Intelligence (AI) tools in the creation of this article.

### Acknowledgements

This study is supported via funding from Prince sattam bin Abdulaziz University project number (PSAU/2024/R/1445).

### Conflict of interest

The authors declare no conflict of interest.

### References

1. A.-M. Wazwaz, Two new integrable fourth-order nonlinear equations: multiple soliton solutions and multiple complex soliton solutions, *Nonlinear Dyn.*, **94** (2018), 2655–2663. <https://doi.org/10.1007/s11071-018-4515-4>
2. A.-M. Wazwaz, W. Alhejaili, S. A. El-Tantawy, Study on extensions of (modified) Korteweg–de Vries equations: Painlevé integrability and multiple soliton solutions in fluid mediums, *Phys. Fluids*, **35** (2023), 093110. <https://doi.org/10.1063/5.0169733>
3. Y. Li, S.-F. Tian, J.-J. Yang, Riemann–Hilbert problem and interactions of solitons in the-component nonlinear Schrödinger equations, *Stud. Appl. Math.*, **148** (2022), 577–605. <https://doi.org/10.1111/sapm.12450>
4. Z.-Q. Li, S.-F. Tian, J.-J. Yang, On the soliton resolution and the asymptotic stability of N-soliton solution for the Wadati-Konno-Ichikawa equation with finite density initial data in space-time solitonic regions, *Adv. Math.*, **409** (2022), 108639. <https://doi.org/10.1016/j.aim.2022.108639>
5. Z.-Q. Li, S.-F. Tian, J.-J. Yang, Soliton resolution for the Wadati–Konno–Ichikawa equation with weighted Sobolev initial data, *Ann. Henri Poincaré*, **23** (2022), 2611–2655. <https://doi.org/10.1007/s00023-021-01143-z>
6. Z.-Q. Li, S.-F. Tian, J.-J. Yang, E. Fan, Soliton resolution for the complex short pulse equation with weighted Sobolev initial data in space-time solitonic regions, *J. Differ. Equations*, **329** (2022), 31–88. <https://doi.org/10.1016/j.jde.2022.05.003>
7. Z.-Q. Li, S.-F. Tian, J.-J. Yang, On the asymptotic stability of N-soliton solution for the short pulse equation with weighted Sobolev initial data, *J. Differ. Equations*, **377** (2023), 121–187. <https://doi.org/10.1016/j.jde.2023.08.028>
8. X.-Y. Gao, Considering the wave processes in oceanography, acoustics and hydrodynamics by means of an extended coupled (2+1)-dimensional Burgers system, *Chinese J. Phys.*, **86** (2023), 572–577. <https://doi.org/10.1016/j.cjph.2023.10.051>

9. X.-Y. Gao, Letter to the Editor on the Korteweg-de Vries-type systems inspired by Results Phys. 51, 106624 (2023) and 50, 106566 (2023), *Results Phys.*, **53** (2023), 106932. <https://doi.org/10.1016/j.rinp.2023.106932>
10. X.-Y. Gao, Y.-J. Guo, W.-R. Shan, Ultra-short optical pulses in a birefringent fiber via a generalized coupled Hirota system with the singular manifold and symbolic computation, *Appl. Math. Lett.*, **140** (2023), 108546. <https://doi.org/10.1016/j.aml.2022.108546>
11. X.-H. Wu, Y.-T. Gao, Generalized Darboux transformation and solitons for the Ablowitz–Ladik equation in an electrical lattice, *Appl. Math. Lett.*, **137** (2023), 108476. <https://doi.org/10.1016/j.aml.2022.108476>
12. Y. Shen, B. Tian, T.-Y. Zhou, C.-D. Cheng, Multi-pole solitons in an inhomogeneous multi-component nonlinear optical medium, *Chaos, Soliton. Fract.*, **171** (2023), 113497. <https://doi.org/10.1016/j.chaos.2023.113497>
13. T.-Y. Zhou, B. Tian, Y. Shen, X.-T. Gao, Auto-Bäcklund transformations and soliton solutions on the nonzero background for a (3+1)-dimensional Korteweg-de Vries-Calogero-Bogoyavlenskii-Schif equation in a fluid, *Nonlinear Dyn.*, **111** (2023), 8647–8658. <https://doi.org/10.1007/s11071-023-08260-w>
14. C. Xu, M. Farman, Z. Liu, Y. Pang, Numerical approximation and analysis of epidemic model with constant proportional caputo(CPC) operator, *Fractals*, in press. <https://doi.org/10.1142/S0218348X24400140>
15. C. Xu, Y. Zhao, J. Lin, Y. Pang, Z. Liu, J. Shen, et al., Mathematical exploration on control of bifurcation for a plankton-oxygen dynamical model owning delay, *J. Math. Chem.*, in press. <https://doi.org/10.1007/s10910-023-01543-y>
16. W. Ou, C. Xu, Q. Cui, Y. Pang, Z. Liu, J. Shen, et al., Hopf bifurcation exploration and control technique in a predator-prey system incorporating delay, *AIMS Mathematics*, **9** (2024), 1622–1651. <https://doi.org/10.3934/math.2024080>
17. Q. Cui, C. Xu, W. Ou, Y. Pang, Z. Liu, P. Li, et al., Bifurcation behavior and hybrid controller design of a 2D Lotka-Volterra commensal symbiosis system accompanying delay, *Mathematics*, **11** (2023), 4808. <https://doi.org/10.3390/math11234808>
18. C. Xu, M. Farman, A. Shehzad, Analysis and chaotic behavior of a fish farming model with singular and non-singular kernel, *Int. J. Biomath.*, in press. <https://doi.org/10.1142/S179352452350105X>
19. W. X. Ma, Complexiton solutions to the Korteweg–de Vries equation, *Phys. Lett. A*, **301** (2002), 35–44. [https://doi.org/10.1016/S0375-9601\(02\)00971-4](https://doi.org/10.1016/S0375-9601(02)00971-4)
20. L. Ma, H. Li, J. Ma, Single-peak solitary wave solutions for the generalized Korteweg–de Vries equation, *Nonlinear Dyn.*, **79** (2015), 349–357. <https://doi.org/10.1007/s11071-014-1668-7>
21. Z.-Y. Ma, J.-X. Fei, J.-C. Chen, Nonlocal symmetry and explicit solution of the Alice-Bob modified Korteweg-de Vries equation, *Commun. Theor. Phys.*, **70** (2018), 031. <https://doi.org/10.1088/0253-6102/70/1/31>
22. X.-Y. Gao, Two-layer-liquid and lattice considerations through a (3+1)-dimensional generalized Yu-Toda-Sasa-Fukuyama system, *Appl. Math. Lett.*, **152** (2024), 109018. <https://doi.org/10.1016/j.aml.2024.109018>

23. X.-Y. Gao, Oceanic shallow-water investigations on a generalized Whitham–Broer–Kaup–Boussinesq–Kupershmidt system, *Phys. Fluids*, **35** (2023), 127106. <https://doi.org/10.1063/5.0170506>
24. L. Tang, Dynamical behavior and multiple optical solitons for the fractional Ginzburg–Landau equation with  $\beta$ -derivative in optical fibers, *Opt. Quant. Electron.*, **56** (2024), 175. <https://doi.org/10.1007/s11082-023-05761-1>
25. L. Tang, A. Biswas, Y. Yıldırım, M. Aphane, A. A. Alghamdi, Bifurcation analysis and optical soliton perturbation with Radhakrishnan–Kundu–Lakshmanan equation, *P. Est. Acad. Sci.*, **73** (2024), 17–28. <https://doi.org/10.3176/proc.2024.1.03>
26. L. Tang, Bifurcations and dispersive optical solitons for the nonlinear Schrödinger–Hirota equation in DWDM networks, *Optik*, **262** (2022), 169276. <https://doi.org/10.1016/j.ijleo.2022.169276>
27. L. Tang, Bifurcation analysis and multiple solitons in birefringent fibers with coupled Schrödinger–Hirota equation, *Chaos, Soliton. Fract.*, **161** (2022), 112383. <https://doi.org/10.1016/j.chaos.2022.112383>
28. A. Sen, D. P. Ahalpara, A. Thyagaraja, G. S. Krishnaswami, A KdV-like advection–dispersion equation with some remarkable properties, *Commun. Nonlinear Sci.*, **17** (2012), 4115–4124. <https://doi.org/10.1016/j.cnsns.2012.03.001>
29. O. González-Gaxiola, J. R. de Chávez, Traveling wave solutions of the generalized scale-invariant analog of the KdV equation by tanh–coth method, *Nonlinear Engineering*, **12** (2023), 20220325. <https://doi.org/10.1515/nleng-2022-0325>
30. S. Saifullah, M. M. Alqarni, S. Ahmad, D. Baleanu, M. A. Khan, E. E. Mahmoud, Some more bounded and singular pulses of a generalized scale-invariant analogue of the Korteweg–de Vries equation, *Results Phys.*, **52** (2023), 106836. <https://doi.org/10.1016/j.rinp.2023.106836>
31. L. Alzaleq, V. Manoranjan, B. Alzalg, Exact traveling waves of a generalized scale-invariant analogue of the Korteweg–de Vries equation, *Mathematics*, **10** (2022), 414. <https://doi.org/10.3390/math10030414>
32. W. W. Mohammed, C. Cesarano, The soliton solutions for the (4+1)-dimensional stochastic Fokas equation, *Math. Method. Appl. Sci.*, **46** (2023), 7589–7597. <https://doi.org/10.1002/mma.8986>
33. Y. Chen, Q. Wang, B. Li, The stochastic soliton-like solutions of stochastic KdV equations, *Chaos, Soliton. Fract.*, **23** (2005), 1465–1473. <https://doi.org/10.1016/j.chaos.2004.06.049>
34. I. Onder, H. Esen, A. Secer, M. Ozisik, M. Bayram, S. Qureshi, Stochastic optical solitons of the perturbed nonlinear Schrödinger equation with Kerr law via Ito calculus, *Eur. Phys. J. Plus*, **138** (2023), 872. <https://doi.org/10.1140/epjp/s13360-023-04497-x>
35. S. U. Rehman, J. Ahmad, T. Muhammad, Dynamics of novel exact soliton solutions to stochastic chiral nonlinear Schrödinger equation, *Alex. Eng. J.*, **79** (2023), 568–580. <https://doi.org/10.1016/j.aej.2023.08.014>
36. O. El-shamy, R. El-barkoki, H. M. Ahmed, W. Abbas, I. Samir, Exploration of new solitons in optical medium with higher-order dispersive and nonlinear effects via improved modified extended tanh function method, *Alex. Eng. J.*, **68** (2023), 611–618. <https://doi.org/10.1016/j.aej.2023.01.053>



37. X. Zhao, B. Tian, D.-Y. Yang, X.-T. Gao, Conservation laws, N-fold Darboux transformation, N-dark-bright solitons and the Nth-order breathers of a variable-coefficient fourth-order nonlinear Schrödinger system in an inhomogeneous optical fiber, *Chaos, Soliton. Fract.*, **168** (2023), 113194. <https://doi.org/10.1016/j.chaos.2023.113194>
38. S. Yasin, A. Khan, S. Ahmad, M. S. Osman, New exact solutions of (3+1)-dimensional modified KdV-Zakharov-Kuznetsov equation by Sardar-subequation method, *Opt. Quant. Electron.*, **56** (2024), 90. <https://doi.org/10.1007/s11082-023-05558-2>
39. M. ur Rahman, M. Alqudah, M. A. Khan, B. E. H. Ali, S. Ahmad, E. E. Mahmoud, et al., Rational solutions and some interactions phenomena of a (3+1)-dimensional BLMP equation in incompressible fluids: A Hirota bilinear method and dimensionally reduction approach, *Results Phys.*, **56** (2024), 107269. <https://doi.org/10.1016/j.rinp.2023.107269>
40. J. Ahmad, Z. Mustafa, S. U. Rehman, N. B. Turki, N. A. Shah, Solitary wave structures for the stochastic Nizhnik–Novikov–Veselov system via modified generalized rational exponential function method, *Results Phys.*, **52** (2023), 106776. <https://doi.org/10.1016/j.rinp.2023.106776>
41. F. Liu, Y. Feng, The modified generalized Kudryashov method for nonlinear space–time fractional partial differential equations of Schrödinger type, *Results Phys.*, **53** (2023), 106914. <https://doi.org/10.1016/j.rinp.2023.106914>
42. P. Li, R. Gao, C. Xu, J. Shen, S. Ahmad, Y. Li, Exploring the impact of delay on Hopf bifurcation of a type of BAM neural network models concerning three nonidentical delays, *Neural Process. Lett.*, **55** (2023), 5905–5921. <https://doi.org/10.1007/s11063-023-11392-0>
43. M. Chinnamuniyandi, S. Chandran, C. Xu, Fractional order uncertain BAM neural networks with mixed time delays: An existence and Quasi-uniform stability analysis, *J. Intell. Fuzzy Syst.*, **46** (2024), 4291–4313. <https://doi.org/10.3233/JIFS-234744>



AIMS Press

©2024 the Author(s), licensee AIMS Press. This is an open access article distributed under the terms of the Creative Commons Attribution License (<http://creativecommons.org/licenses/by/4.0>)